Theoretical modelling and experimental study of novel photothermal microactuators

Lihong Ma (马利红)[1,2], Dongxian Zhang (张冬仙)[1*], Chao Liu (刘 超)[1], and Haijun Zhang (章海军)[1]

[1] *State Key Laboratory of Modern Optical Instrumentation, Zhejiang University, Hangzhou 310027, China*

[2] *Information Optical Institute, Zhejiang Normal University, Jinhua 321004, China*

[*] *E-mail: zhangdx@zju.edu.cn*

Received November 11, 2008

We present a category of novel photothermal (PT) microactuators. Each microactuator consists of two PT arms that are jointed at the free end and connected to an anchor at the fixed end. When a laser beam irradiates one of the arms (called hot arm, and the other is cold arm), light energy is absorbed and converted into heat. The asymmetric thermal expansion of the hot and cold arms results in lateral deflection. Based on conduction heat transfer theory and heat dissipation mechanism, we study the PT effects and establish the theoretical model of PT expansion for the microactuators. The temperature distribution and the linear thermal expansion can be numerically calculated. The analytical solution provides an insight into the operation of the actuators and predicts the performance of the actuators with new designs. A symmetry microactuator and a microswitch as the prototypes have been fabricated and tested. The experimental results are in good agreement with the theoretical predictions and prove the feasibility of the novel PT microactuators.

OCIS codes: 120.6780, 350.5340, 220.4000, 230.3990, 140.3460.

doi: 10.3788/COL20090708.0694.

Microactuators are the key devices of micro-electro-mechanical system (MEMS). So far, a variety of micro drive designs exploiting motion obtainable have been reported. They are designed using several kinds of actuation mechanisms such as electrostatic, piezoelectric, photoelectric, magnetostrictive, magnetic, and thermo-mechanical actuations[1−7]. Among these types of actuators, electro-thermal microactuators, due to their compact structure and large displacement output, have been widely applied in many fields ranging from telecommunication to medicine. Generally, electro-thermal actuators are excited by Joule heat from flowing current in resistor. Drive voltage is provided by embedded small battery or external power supply source connected to microactuators through wires. The former will limit the miniaturization and the life of actuators. The latter will affect the mobility of the whole device.

As an alternative, photothermal (PT) microactuator can be considered since it uses laser light source as an external wireless power supply. This method can remove the constraints of electro-thermal microactuators mentioned above. What's more, it enables noncontact motion control and remote operation in a special environment such as chamber or electrical isolation. Therefore, the PT microactuators have gained much attention. Han *et al*. reported a double-layer actuator[8]. Oliver *et al*. reported two kinds of actuators with four-layer structure fabricated by using the SUMMiTV polysilicon surface micro-machining process[9]. Szabo *et al*. reported a photothermally activated V-shape polysilicon actuator for micro-robots[10]. Zhang *et al*. observed the PT expansion using a light microscope system combined with a charge-coupled device (CCD)[11].

In this letter, we present a category of novel PT microactuators. They are made of single layer material with different topologies and shapes, and fabricated by an excimer laser machining workstation. Each microactuator consists of a hot arm and a cold arm, which are jointed at the free end and connected to an anchor at the fixed end. While a laser beam irradiates one of the microactuator's arms, light energy is absorbed and converted into heat. The asymmetric thermal expansion of the hot and cold arms results in lateral deflection. Based on conduction heat transfer theory and heat dissipation mechanism, we investigate the PT effects and establish a theoretical model of PT expansion for the microactuators. The values of linear thermal expansion are numerically calculated. The analytical solution can provide an insight into the operation and performance of the actuators with new designs. A symmetric microactuator and a microswitch as the examples have been fabricated and tested. The experimental results are in good agreement with theoretical predictions.

The schematic diagram of a symmetric PT microactuator is shown in Fig. 1. The thickness of the arm we designed is thin enough to satisfy $Bi \ll 1$ (Bi refers to Biot number), thus it is reasonable to assume a uniform temperature distribution along the direction of thickness, which means we only consider the temperature distribution in a plane that has two dimensions of width and length. In Fig. 1, laser irradiates one of the arms. Since the width of the bridge and the gap are so small that the heat flux through them is little, we need only analyze the hot arm irradiated by laser. In addition, when the length of the arm is much greater than the width and the laser spot size is comparable to the width, the PT response of the arm can be simplified for analysis in one dimension. In fact, we have studied the temperature distribution of the two-dimensional (2D) model of the arm using finite element simulation method. The result shows that, under

 © 2009 Chinese Optics Letters

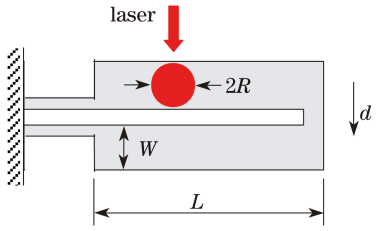

Fig. 1. Schematic diagram of a symmetric PT microactuator.

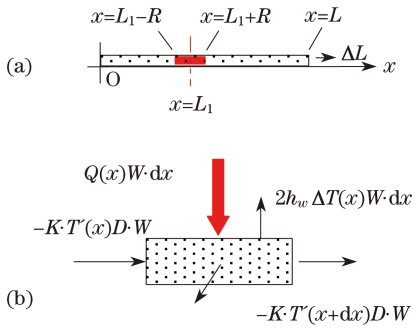

Fig. 2. Theoretical analysis model. (a) Simplified 1D coordinate system of the hot arm; (b) differential element of the hot arm.

the above conditions, the one-dimensional (1D) model is reasonable. Figure 2(a) shows the simplified 1D coordinate system of the hot arm. Figure 2(b) is a differential element of the hot arm.

PT microactuators use laser light as the heat source supply. When laser irradiates the microactuator, part of the optical energy will be absorbed and converted into the heat energy. Though the general type of laser beam is Gaussian, we have learnt from the numerical solution that the difference in laser energy distribution only slightly affects the temperature distribution in the irradiated zone and scarcely affects the temperature distribution of the whole arm. Therefore, the power density distribution of incident laser can be assumed as constant. In 1D model, the heat power density due to the light absorption is approximately expressed as

$$Q(x) = \begin{cases} \rho_{\mathrm{A}} q_0, & L_1 - R \le x \le L_1 + R \\ 0, & x < L_1 - R, x > L_1 + R \end{cases}, \tag{1}$$

where q_0 is the incident laser power density, ρ_{A} is the ratio of absorption, R is the radius of the laser spot, and L_1 is the coordinate of the center of the laser spot.

When the arm is heated, it will lose heat in two mechanisms of convection and radiation[12]. At lower temperature, convection is the dominating mechanism; at higher temperature, irradiative losses become important. The temperature is limited to be under the melting point of polymer material, so in our analysis, we can ignore the energy loss through irradiation. The heat flow equation is derived by examining differential element of the arm of width W, thickness D, and length $\mathrm{d}x$, as shown in Fig. 2(b). Under steady-state conditions, the heating power generated in the element is equal to heat conduction and heat convection out of the element:

$$\begin{aligned} &-KT'(x)DW + Q(x)W \cdot \mathrm{d}x = \\ &-KT'(x+\mathrm{d}x)DW + [T(x) - T_0]\cdot \\ &(2Wh_w \cdot \mathrm{d}x + 2Dh_D \cdot \mathrm{d}x), \end{aligned} \tag{2}$$

where $T(x)$ is the temperature distribution when the arm is irradiated, T_0 is the environment temperature, K is the thermal conductivity of the material, h_D is the coefficient of the convective heat transfer on the side wall, and h_w is the coefficient of the convective heat transfer on the up and down surfaces (under the sub-millimeter scale, both of the h_w can be assumed to be the same). Taking the limit as $\mathrm{d}x \to 0$ for Eq. (2) produces the following second-order differential equation:

$$\frac{\mathrm{d}^2 T(x)}{\mathrm{d}x^2} - \frac{2(h_D D + h_w W)}{KDW} \cdot [T(x) - T_0] = -\frac{Q(x)}{KD}. \tag{3}$$

Physically, the first term on the left side of Eq. (3) represents the net rate of heat conduction into the element per unit volume. The second term on the left side is the rate of the heat energy loss in the element per unit volume. The right side represents the rate of heat energy input into the element per unit volume.

The width of the bridge is so small that the heat flux from the hot arm to it can be regarded as zero. So both ends of the arm, where $x = 0$ and $x = L$, can be assumed to be contact ends with air. Under steady-state conditions, both ends are considered to have the same temperature as the ambient air. According to the coordinate system shown in Fig. 2(a), the thermal boundary conditions can be expressed as

$$T(0) = T_0, \quad T(L) = T_0. \tag{4}$$

We change the variables for Eq. (3) with

$$\Delta T = T - T_0, \tag{5}$$

ΔT denotes the temperature rising. Solving Eq. (4) with the boundary conditions, we can obtain the rising temperature distribution as

$$\Delta T(x) = \begin{cases} \frac{2\rho_{\mathrm{A}} q_0 \mathrm{sh}(bR)}{KDb^2 \mathrm{sh}(bL)} \mathrm{sh}[b(L - L_1)]\mathrm{sh}(bx), \\ \qquad\qquad 0 \le x \le L_1 - R \\ \frac{2\rho_{\mathrm{A}} q_0 \mathrm{sh}(bR)}{KDb^2 \mathrm{sh}(bL)} \mathrm{sh}[b(L - L_1)]\mathrm{sh}(bx) \\ -\frac{\rho_{\mathrm{A}} q_0}{KDb^2} \{\mathrm{ch}[b(x + R - L_1)] - 1\}, \\ \qquad\qquad L_1 - R \le x \le L_1 + R \\ \frac{2\rho_{\mathrm{A}} q_0 \mathrm{sh}(bR)}{KDb^2 \mathrm{sh}(bL)} \mathrm{sh}[b(L - L_1)]\mathrm{sh}(bx) \\ -\frac{2\rho_{\mathrm{A}} q_0}{KDb^2} \mathrm{sh}(bR)\mathrm{sh}[b(x - L_1)], \\ \qquad\qquad L_1 + R \le x \le L \end{cases} \tag{6}$$

with

$$b^2 = \frac{2(h_D D + h_w W)}{KDW}. \tag{7}$$

The temperature rising will produce linear PT expansion. When the thermal expansion coefficient of the material α is given, the linear expansion for the arm can be calculated by

$$\begin{aligned} \Delta L &= \alpha \int_0^L \Delta T(x)\mathrm{d}x \\ &= \alpha \frac{2\rho_{\mathrm{A}} q_0 R}{KDb^2} - \alpha \frac{2\rho_{\mathrm{A}} q_0}{KDb^3} \mathrm{sh}(bR)\mathrm{ch}[b(L - L_1)] \\ &\quad - \alpha \frac{2\rho_{\mathrm{A}} q_0}{KDb^3 \mathrm{sh}(bL)} \mathrm{sh}(bR)\mathrm{sh}[b(L - L_1)][1 - \mathrm{ch}(bL)]. \end{aligned} \tag{8}$$

Equation (8) interprets the relationship between the PT expansion and the geometric parameters of the microactuator and the physical properties of the material.

The equation also demonstrates that the PT expansion is approximately proportional to the incident light power density. In addition, the location of the laser spot might also affect the expansion, even though this influence is proved to be slight. The PT expansion is then converted into enlarged lateral deflection of the actuator.

For the PT arm within a microactuator, when the irradiating laser is determined (including the power, wavelength, size, and location of the spot) and the geometric parameters and physical properties of the arm are given, the value of PT expansion can be uniquely determined.

Table 1 shows the parameters of the laser and the PT arm of the symmetric microactuator studied in this letter. According to Eq. (8) and Table 1, the analytical relationship between the expansion ΔL and the laser power P_0 ($P_0 = q_0 \cdot \pi R^2$) can be worked out, as demonstrated in Fig. 3. The results indicate that the PT expansion grows with the increase of laser power, and is approximately linear with the power. When the power is 10 mW, the theoretical value of PT expansion may reach 1.57 μm.

Table 1. Parameters of Laser and PT Arm of the Microactuator

Name	Description	Given Value
R	Radius of Laser Spot	50 μm
P_0	Laser Power	0−10 mW
λ	Laser Wavelength	650 nm
$\rho_{\rm A}$	Rate of Absorption	0.8
L_1	Coodinate of the Laser Spot Center	150 μm
L	Length of the Arm	570 μm
W	Width of the Arm	100 μm
D	Thickness of the Arm	40 μm
K	Thermal Conductivity of the Material	0.24 W/(m·K)
α	Thermal Expansion Coefficient of the Material	32×10^{-6} K^{-1}
h_D	Coefficient of the Convective Heat Transfer on the Side Surface	500 W/(mm^2·K)
h_w	Coefficient of the Convective Heat Transfer on the Up or Down Surface	30 W/(mm^2·K)
T_0	Initial Temperature (Environment Temperature) of the Arm	23 °C

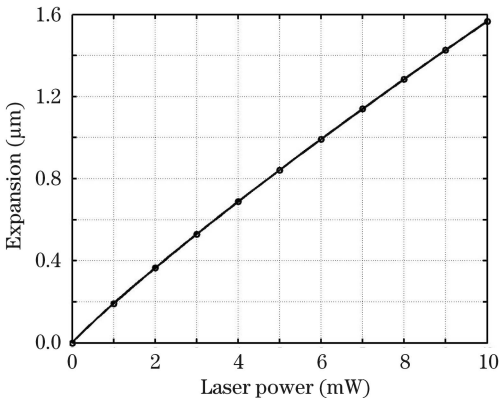

Fig. 3. Theoretical relationship between the PT expansion and the laser power.

Like other microactuators, such as the bi-directional electrothermal actuators, the bi-directional PT actuator is able to convert and enlarge longitudinal PT expansion ΔL into lateral deflection d. Therefore, we designed and fabricated a symmetric PT microactuator by a high performance and multifeatured excimer laser workstation (Optec Promaster, Belgium). The excimer laser workstation is one of the most popular tools for micromachining microstructures with feature width range of 1−1000 μm for many kinds of materials including polymers, metal, and ceramics, etc. Optec Promaster can load $*$. dxf format file exported from AutoCAD in Version 14 or later and handle the material automatically according to the vector graph of the file.

Black polyethylene material, which has larger optical absorption ratio and high thermal expansion coefficient, was used to fabricate the microactuators. Figure 4 is a microscopic image of the machined symmetric microactuator. A built-in scale next to the microactuator tip was introduced to indicate its deflection. An embroidery needle adjacent to the microactuator is imaged for comparison to show that the actuator is quite small. The geometric dimension parameters of the microactuator are as follows: two 570-μm-long, 100-μm-wide arms; two 175-μm-long, 10-μm-wide bridges; a 50-μm-long, 36-μm-wide cross section gap; 40-μm thickness.

The theoretical analysis has shown that the performance of a PT microactuator is related to the physical parameters and geometry as well as incident laser power, laser spot size, and the location of the laser spot. Here we only present the relationship between the lateral deflection and laser power. Other performances such as the relationship between PT deflection and laser frequency will be studied and discussed elsewhere.

We used a laser diode with output wavelength of 650 nm and maximum output power of 10 mW to irradiate the actuator. The diameter of laser beam cross section was about 100 μm. The actuator generated lateral deflection toward the cold arm side, as shown in Fig. 5.

All experiments were monitored by a CCD-combined light microscope system. For briefness, Fig. 5 only shows three typical states of the PT deflection. The upper images are snapshots from videos using a 4× objective

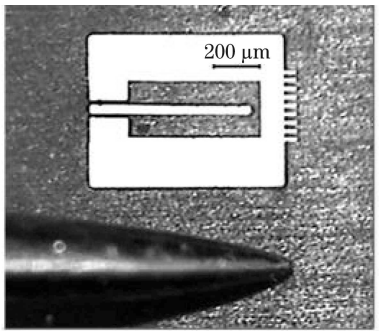

Fig. 4. Microscopic image of the symmetric PT microactuator.

lens, while the zoomed images (lower rows) are snapshots from videos using a 16× objective lens. We can precisely measure the data of lateral deflection of microactuators by using a self-designed sub-pixel video analysis software.

According to the principle of sub-pixel measurement, the measurement resolution of our microscope system and software is on the scale of sub-pixel, which depends on the image magnification and CCD detector resolution. The pixel size of microscopic images captured using a 16× objective lens is about 0.75 μm, therefore, the sub-pixel measurement resolution is on the scale of around 0.1 μm.

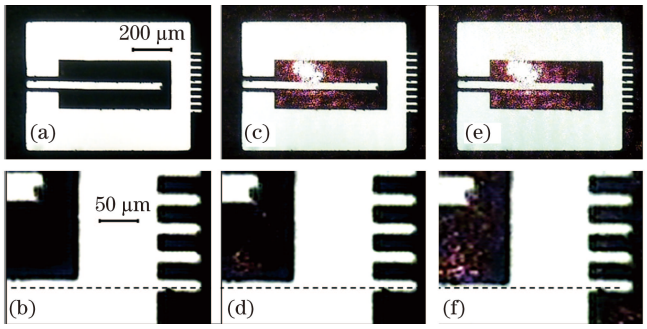

Fig. 5. Microscopic images show how the symmetric microactuator deflects. (a) Original state without irradiation, (b) zoomed part of (a); (c) PT deflection of microactuator when irradiated by 3-mW laser, (d) zoomed part of (c); (e) deflection of microactuator at 10-mW laser, (f) zoomed part of (e).

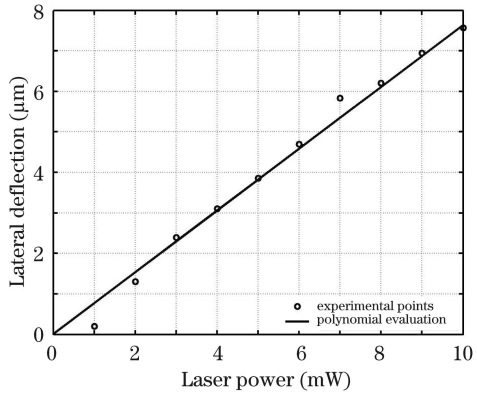

Fig. 6. Experimental relationship between the PT deflection and the laser power.

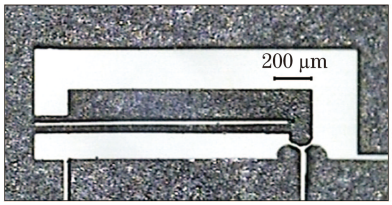

Fig. 7. Microscopic image of the microswitch-like PT actuator.

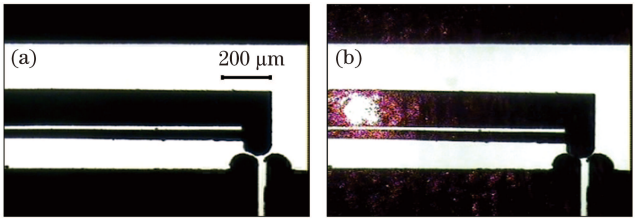

Fig. 8. Microscopic images show how the microswitch-like actuator works. (a) Original state, (b) deflecting and switching state when irradiated.

Figures 5(a) and (b) show the original state of the microactuator, Figs. 5(c) and (d) display the deflecting state under 3-mW laser power with a PT deflection of 2.4 μm, while Figs. 5(e) and (f) display the state at 10 mW with a deflection of 7.6 μm. To exploit the relationship between the PT deflection and laser power, we measured a series of lateral deflection values under different laser powers. Experimental data and linear fitting curve are given in Fig. 6.

It is clearly indicated that the PT deflection increases with the rise of laser power, and is approximately linearly proportional to the power. Moreover, at the laser power of 10 mW, the numerical expansion is 1.57 μm (see Fig. 3), while the measured lateral deflection reaches 7.6 μm, with a magnification of 4.8. The result further proves the feasibility of enlarging longitudinal PT expansion into lateral deflection. Comparing Fig. 6 with Fig. 3, we may find that the experimental data and curve agree well with the theoretical predictions, for both curves are nearly of the same shape and trend.

As an example of application, we next designed and fabricated a microswitch-like PT actuator (Fig. 7). When irradiated by a periodic laser pulse, the actuator will switch on and off alternately. Figure 8 provides the images captured from the microscopic videos. Figure 8(a) shows the original state of the microswitch, Fig. 8(b) shows the deflecting and switching state when irradiated. With this method, we may develop various microswitches utilizing PT expansion and deflection.

In conclusion, through theoretical analysis and mathematical derivation, a comprehensive model has been developed to describe the characteristics of PT expansion and deflection, and to make the theoretical predictions about the relationship between the expansion/deflection and the laser power. Both the theoretical and experimental results show that the PT expansion is nearly linear with the laser power. Some typical PT microactuators have been fabricated and tested. The experimental results prove the feasibility of the PT microactuator, and are in good agreement with the theoretical predictions. Such kinds of PT microactuators have more advantages than previous types of actuators. Firstly, the actuators can be simply made of single layer materials rather than multi-layer ones, and we may employ a variety of conductive or non-conductive materials. In this case, its in-plane deflection eliminates shearing forces between different layers, which may cause influence to the life of microactuator. Secondly, it enables wireless and remote control without any electric or electronic connection, and easier integration or miniaturization becomes practical and feasible. Thirdly, it may generate larger output for the same input power due to larger thermal expansion coefficient and optical absorption coefficient of polymer material. As already mentioned, by using a laser power of only 10 mW, we may obtain a 7.6-μm PT deflection. Deflection in such an order is generally sufficient for most of the practical micro/nano applica-

tions. The PT microactuators provide a novel method of microactuation for MEMS or micro/nano-technologies.

This work was supported by the National "863" Program of China (No. 2006AA04Z237) and the National Natural Science Foundation of China (No. 50775205).

References

1. A. Selvakumar and K. Najafi, J. Microelectromech. Syst. **12,** 440 (2003).
2. J.-C. Shen, W.-Y. Jywe, H.-K. Chiang, and Y.-L. Shu, Prec. Eng. **32,** 71 (2008).
3. N. Kawashima, K. Takeda, and K. Yabe, Chin. Opt. Lett. **5,** S109 (2007).
4. Y.-W. Park and D.-Y. Kim, J. Magn. Magn. Mater. **272−276,** e1765 (2004).
5. S. Fu, G. Ding, H. Wang, Z. Yang, and J. Feng, Microelectron. Journal **38,** 556 (2007).
6. Q.-A. Huang and N. K. S. Lee, J. Micromech. Microeng. **9,** 64 (1999).
7. Z. Han, C. Zhou, and E. Dai, Chin. Opt. Lett. **6,** 619 (2008).
8. L.-H. Han and S. Chen, Sensors and Actuators A **121,** 35 (2005).
9. A. D. Oliver, S. R. Vigil, and Y. B. Gianchandani, IEEE Trans. Electron Devices **50,** 1156 (2003).
10. F. R. Szabo and P. E. Kladitis, in *Proceedings of the 2004 International Conference on MEMS NANO and Smart Systems* 446 (2004).
11. D. Zhang, H. Zhang, C. Liu, and J. Jiang, Microsc. Res. Techn. **71,** 119 (2008).
12. N. D. Mankame and G. K. Ananthasuresh, J. Micromech. Microeng. **11,** 452 (2001).